CRYOGENIC FLUID JET DYNAMICS AT SUPERCRITICAL CONDITIONS

Nan Zong, Shanwu Wang and Vigor Yang
Department of Mechanical & Nuclear Engineering
The Pennsylvania State University
University Park, PA 16802, *USA*
zongnan@psu.edu; shanwu@psu.edu; vigor@psu.edu

ABSTRACT

Injection of cryogenic fluid initially at a subcritical temperature into a supercritical environment has been investigated numerically. The model accommodates full conservation laws and real-fluid thermodynamics and transport phenomena. All of the thermophysical properties are determined directly from fundamental thermodynamic theories and the corresponding state principles. The resultant scheme is valid for the entire fluid states of concern. Turbulence closure is achieved using a large-eddy-simulation technique. As a specific example, the dynamics of a liquid nitrogen stream injected into a supercritical nitrogen environment has been studied systematically over a broad range of ambient pressure. Owing to the large property variations from the injected and surrounding fluids, a string of strong density-gradient regimes is generated around the jet surface and exerts a stabilizing effect on the flow evolution. The situation becomes more evident with decreasing pressure. The kinetic energy of the surface motion is transferred from its vertical to the horizontal component; the instability waves are effectively suppressed. The jet dynamics is largely dictated by the local thermodynamic state. When the fluid temperature transits from the sub- to the super-critical value, the rapid property variations may qualitatively change the jet behavior compared with its counterpart at low pressures.

INTRODUCTION

Injection of liquid fluid initially at a subcritical temperature into an environment in which the temperature and pressure exceed the thermodynamic critical point is an important phenomenon in many high-pressure combustion devices, including diesel, gas-turbine, and liquid-propellant rocket engines. Under these conditions, fluid jets exhibit many characteristics distinct from their counterparts at low pressures. First, because of the diminishment of surface tension and enthalpy of vaporization, the sharp distinction between the liquid and gas phases vanishes. The fluid properties and their spatial gradients vary continuously throughout the entire field. Second, thermodynamic and transport anomalies may occur during the temperature transition from the sub- to the super-critical value, especially when the pressure approaches the critical point, a phenomenon commonly referred to as the near-critical enhancement (Levelt Senger, 1991). As a result, the compressibility effects (i.e., volumetric changes induced by pressure variations) and variable inertial effects (i.e., volumetric changes induced by heat addition and/or variable composition) play an important role in dictating the flow evolution. Third, the characteristic times of the flow motions around the jet boundary have the same order of magnitude at supercritical conditions. The resultant coupling dynamics becomes transient in both the jet interior and the surrounding fluid, and subsequently yields an array of physiochemical processes that are dominated by widely disparate time and length scales. Fourth, the flow Reynolds number increases almost linearly with pressure. For oxygen and hydrogen, an increase in pressure from 1 to 100 atmospheres result in a reduction of the corresponding kinematical viscosity by a factor of two orders of magnitude. Based on the Kolmogorov universal equilibrium theory, the Kolmogorov and Taylor microscales may decrease by 1.5 and 1.0 orders of magnitude, respectively. These reductions of characteristic scales of turbulent motions have a direct impact to the flow evolution and the numerical grid density required to resolve key processes (Oefelein and Yang, 1998). Comprehensive reviews of the state of knowledge on supercritical mixing and combustion were recently given by Yang (2000) and Bellan (2000).

Experimental investigation into supercritical fluid jet dynamics dates back to 1971. Newman and Brzustowski (1971) studied the injection of CO_2 fluid with an inlet temperature of 295K into a chamber filled with CO_2 and N_2 mixtures at near critical conditions. The critical temperature and pressure of CO_2 are 304 K and 73 atm, respectively, those of N_2 are 126 K and 34 atm, respectively. The chamber temperature and pressure were preconditioned in the range of 295-330 K and 62-90 atm, respectively, and the CO_2 mass fraction varied from 0 to 50%. A shadowgraph visualization technique was employed to investigate the jet flow evolution and its interaction with the surrounding fluid. Results indicate that over the pressure range considered, the jet surface structure and spray formation were suppressed with increasing temperature and CO_2 concentration in the chamber, mainly due to the diminished surface tension and enhanced CO_2 evaporation at near and above the critical temperature. Droplets were observed around the jet boundary, but their sizes decreased with an increase in the ambient temperature. The jet could be globally treated as a variable-density, single-phase turbulent submerged jet at both subcritical and supercritical pressures, when the ambient temperature remained supercritical.

Motivated by the development of high-pressure cryogenic-propellant rocket engines, extensive experimental studies have recently been conducted to provide direct insight into supercritical fluid injection and mixing. The work included injection of liquid nitrogen and co-injection of

Proceeding of Third International Symposium on Turbulent and Shear Flow Phenomena

liquid nitrogen and gaseous helium into gaseous nitrogen environments over a wide range of pressure (Mayer et al., 1996; Chehroudi et al., 2002a). Cryogenic propellants such as liquid oxygen and hydrogen under both cold-flow and hot-fire test conditions were also considered (Mayer et al., 1996). Results from the shadowgraph images confirmed the findings by Newmman and Brzustowski (1971). Drastic changes in jet surface phenomena took place across the critical pressure. The formation of ligaments and droplets were observed at subcritical pressures; however, these structures disappeared at supercritical pressures due to the predominant influence of turbulence with vanished surface tension. As the ambient pressure exceeds the critical point, the jet changes its appearance to bear a stronger resemblance to gaseous jets. Furthermore, the spatial growth rate of a supercritical cryogenic jet agrees with that of an imcompressible variable-density gaseous jet. The spontaneous Raman Scattering technique was also employed to measure the density field (Oschwald and Schik, 1999; Chehroudi et al., 2000). In general, the normalized density profiles indicated a tendency towards the self-similarity solution observed for classical constant- and variable-density single-phase fluid jets at near and supercritical pressures. The interactions of acoustic waves with a cryogenic nitrogen jet were studied by Chehroudi and colleagues (2002b). It was found that the jet was strongly affected by acoustic waves (4000Hz) at sub-critical conditions. The effects, however, became unnoticeable at super-critical conditions, a phenomenon that may be attributed to the formation of high-frequency vortices on a supercritical jet.

In parallel to experimental studies, attempts were made both theoretically and numerically to provide direct insight. Oefelein and Yang (1998) modeled two-dimensional mixing and combustion of oxygen and hydrogen streams at supercritical conditions by means of a large-eddy-simulation technique. The formulation accommodates real-fluid thermodynamics and transport phenomena. In particular, all the thermophysical properties were evaluated directly from fundamental thermodynamic theories over the entire regime of fluid states of concern. A unified treatment of numerical algorithms based on general fluid thermodynamics was also established to improve computational accuracy and efficiency (Meng and Yang, 2003). Bellan and colleagues (2002) treated the temporal evolution of heptane/nitrogen and oxygen/hydrogen mixing layers at supercritical conditions. Several important characteristics of high-pressure transitional mixing processes were identified. In particular, as a result of the strong-density stratification, the mixing layer is considerable more stable than a corresponding gaseous mixing layer. Energy dissipation due to both the species-flux and heat-flux effects prevail during the evolution of the mixing layer; whereas the viscous effects appears minimal.

The purpose of the present work is to establish a unified model capable of treating the following characteristics of a supercritical jet flow: 1) thermodynamics of high-pressure fluid; 2) near critical transport property anomalies; 3) turbulent mixing over a wide range of scales; and 4) strong property gradients between the injected and surrounding fluids. The theoretical formulation accommodates full conservation laws and real-fluid thermodynamics and transport phenomena. Turbulence closure is achieved using a large-eddy-simulation technique. As a specific example, the injection and mixing of cryogenic nitrogen into a supercritical gaseous nitrogen environment is studied over a wide range of pressure.

THEORETICAL FORMULATION AND NUMERICAL METHOD

The analysis accommodates full conservation laws and real-fluid thermodynamics and transport over the entire temperature and pressure regimes of concern. Turbulence closure is achieved using a large-eddy-simulation (LES) technique, in which large energy-carrying structures are computed explicitly and the effect of small-scale motions on the resolved scales is modeled (Oefelein and Yang, 1998). A Smagorinsky model extended to compressible flow is used to treat the small-scale motions. Thermodynamic properties, including enthalpy, internal energy, and heat capacity, are directly calculated by means of fundamental thermodynamic theories and a modified Soave-Redlich-Kwong (SRK) equation of state that is reasonably accurate over the high-pressure and low temperature regime in the present study and ease of implementation (Yang, 2000). Transport properties, such as viscosity and thermal conductivity, are estimated with an extended corresponding-state principle. Mass diffusivity is obtained by the Takahashi method calibrated for high-pressure conditions. Numerical implementation includes a preconditioning scheme in conjunction with a dual time-stepping integration algorithm (Hsieh and Yang, 1997). All of the numerical relations, including the Jacobian matrices and eigenvalues, are derived based on the same equation of state to render a self-consistent and robust algorithm (Meng and Yang, 2003). Further efficiency is achieved by utilizing a parallel computation scheme that involves the message-passing interface (MPI) library and multi-block treatment.

RESULTS AND DISCUSSION

The injection of cryogenic nitrogen fluid into a supercritical gaseous nitrogen environment is studied in this work. The temperature of the injected nitrogen is 120K, and that of the ambient gaseous nitrogen remains at 300K. The ambient pressure ranges from 42 to 93 atm. Since the critical pressure and temperature of nitrogen are 34 atm and 126 K, respectively, the ambient environment is at supercritical conditions. Cryogenic nitrogen fluid is injected through a circular injector with a diameter of 254 μm. A fully developed turbulent pipe flow with a bulk velocity of 15m/s is assumed at the injector exit. The detailed simulation conditions are presented in Table 1.

Table 1 Test conditions

	Case 1	Case 2	Case 3
u_{in} (m/s)	15	15	15
T_{in} (K)	120	120	120
T_{∞} (K	300	300	300
ρ_{in}(kg/m^3)	563	603	626
ρ_{∞}(kg/m^3)	46	77	103
p_{∞} (MPa)	4.3	6.9	9.3
Re	25700	26700	28800

For a constant-density jet, the shear layer between the jet and the ambient fluid is susceptible to the Kelvin-Helmholz instability and may experience vortex rolling, paring, and breakup. When those three-dimensional instability waves are amplified further downstream, the flow transits from laminar to turbulence. A cryogenic supercritical jet may undergo the same transitional process, but with additional mechanisms including volume dilation and baroclinic torque.

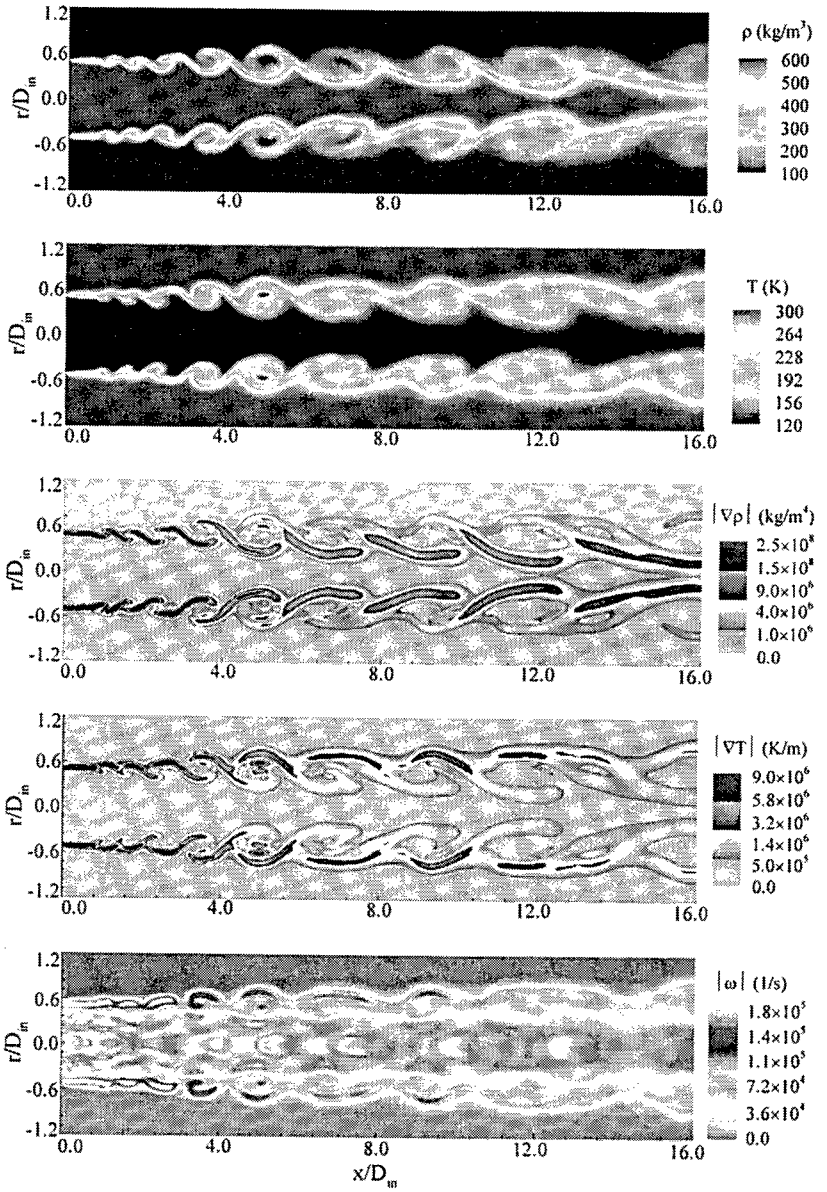

Fig. 1 Snapshots of density, temperature, density-gradient, temperature-gradient and vorticity fields of nitrogen fluid injected at supercritical conditions (p_∞=9.3 MPa, T_∞=300 K, u_{in}= 15 m/s, T_{in}= 120 K, t=1.550 ms, D_{in}=254μm).

Figure 1 shows the snapshots of the instantaneous temperature, density, density-gradient, temperature-gradient and vorticity fields of Case 1. The vortex shedding process can be clearly observed in both the density and temperature fields. Due to hydrodynamic instability, small ripples appear on the jet surface near the injector exit. As those instability waves move downstream, they grow up and roll into a succession of ring vortices. The vortex may interact with the wave behind it and merge together, a process called vortex paring. As a result, , the length scales of vortices increase.

As stated by Crow and Champagne (1971), the evolution and interaction of large coherent structures strongly influence the mixing and entrainment of a mixing layer. In Fig. 1, the lighter and warmer ambient gaseous nitrogen is introduced into the cold nitrogen jet through vortex motion. Furthermore, the density field exhibits a series of thread-like entities emerging from the jet surface. Those kinds of thread- or finger-like structures were also reported in the experiments by Chehroudi and his colleagues for the same test condition. The agreement between the numerical simulation and experimental visualization is encouraging.

In addition to the initial density stratification, a series of large density-gradient regions exist in the flowfield as a result of turbulent entrainment and mixing. To study their effects on the flow evolution, we present the power spectral densities (PSD) of both the axial and radial velocity fluctuations at different locations away from jet centerline. Figure 2a shows that the axial velocity fluctuation increases in the low frequency regime (large scale structures) as the distance from the large density gradient regions decreases, whereas the trend for the radial velocity fluctuation reverses (Fig. 2b). Figure 2b indicates that the radial velocity

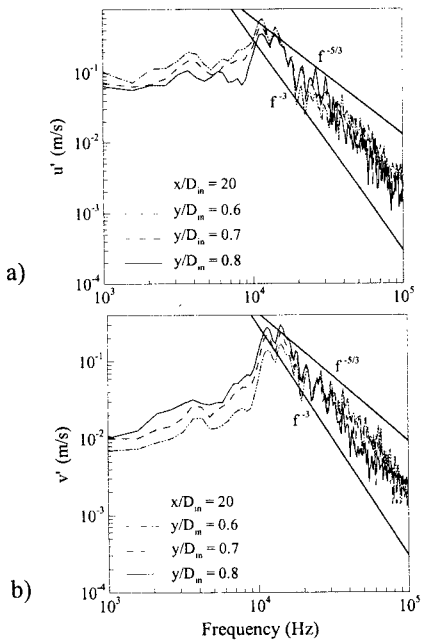

Fig. 2 Power spectral densities of velocity fluctuations at different radial locations (Case 3).

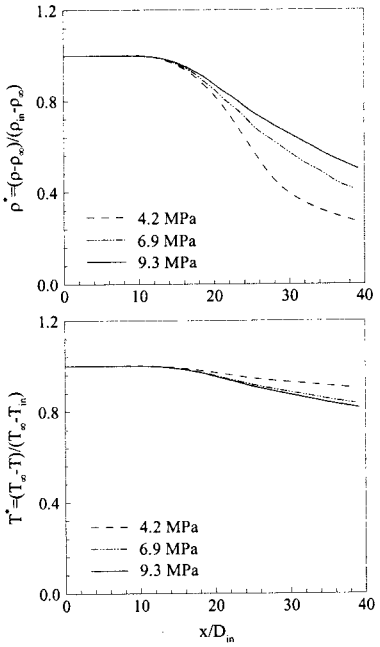

Fig. 4 Effect of pressure on normalized density and temperature distributions along jet centerline.

fluctuation decreases in the low frequency region when the distance from the large density gradient regions decreases. In both figures, the high frequency velocity fluctuations remain basically unaffected. The large-scale low frequency structures are most influenced by the large density gradient regions, which act like a solid wall in the flow that amplifies the axial turbulent fluctuation but damps the radial one. A similar phenomenon was observed by Hannoun et al. (1988) in their experimental work on grid induced shear-free turbulence near the sharp density interface. They argued that because the strong anisotropic nature of the turbulence near the density interface, large eddies of integral length scale tend to flatten at a density interface, which may transfer the kinetic energy from the vertical to the horizontal velocity component. Because of the redistribution of kinetic energy among its spatial components, the '*available energy for mixing*' is much less than the total kinetic energy content near the jet boundary. Therefore, the strong density stratification in the flowfield may damp the radial velocity fluctuation and inhibit the development of the instability wave.

Figures 3 shows the snapshots of the instantaneous density and temperature fields at three different ambient pressures. Since the ambient pressure of Case 1 is closer to the critical pressure, the density stratification between the injected fluid and the ambient gaseous nitrogen is stronger in this case. Consequently, the velocity perturbations in the radial direction are more apt to be damped. The jet surface is nearly straight near the injector, and only very tiny instability waves can be observed around the jet surface in the downstream region. As the ambient pressure increases, the density stratification decreases, so dose the damping effect. The strength of the velocity perturbations in the radial direction thus increases. In Cases 2 and 3, a series of instability waves around the jet surface are generated in the near-injector region, which are amplified as the injected fluid moves downstream. Compared with Case 3, the instability waves generated in Case 2 are relatively weaker and damped further downstream. In both Cases, a series of finger or thread like entities emerge from the jet surface, as evidenced in the experimental observations (Chehroudi et al. 2002a). In addition, temperature field clearly shows the entrainment of hot ambient gaseous nitrogen into the injected fluid due to the motion of vortices. Figure 3 also presents the density-gradient and vorticity fields for all three cases. In Case 1, the initial density stratification layer is slightly stretched by vortex motion. In both Cases 2 and 3, the initial density stratification regions are largely stretched by the interaction and motion of vortices. A string of large coherent structures are clearly observed in those two cases. However, there is still a small difference between the density- gradient field of Cases 2 and 3. Since the damping effect in Case 3 is weaker than that in Case 2, the vortex generated in Case 3 is relatively stronger. Thus, the large coherent structures generated in Case 3 deform more severely in the radial direction than that of Case 2. The vorticity field indicates that the initial shear layer is stretched by the vortex motion in both Cases 2 and 3.

Figure 4 presents the normalized temperature and density distributions along the jet centerline for the three cases. Evidently, the normalized temperature of Case 1 decreases (as the absolute temperature increases) relatively slower along the jet centerline than that of Case 2 and 3. A possible explanation is given below. As is well known, when the temperature and pressure of the injected fluid reach the critical point, the constant pressure specific heat (C_p) may increase to infinite and the thermal diffusivity ($\alpha = k/\rho \cdot C_p$) may decrease to zero, a phenomena known as the near critical slow-down. Because the ambient pressure for Case 1 is close to the critical pressure, the constant pressure specific heat (C_p) of nitrogen increases sharply when the temperature approaches the critical temperature.

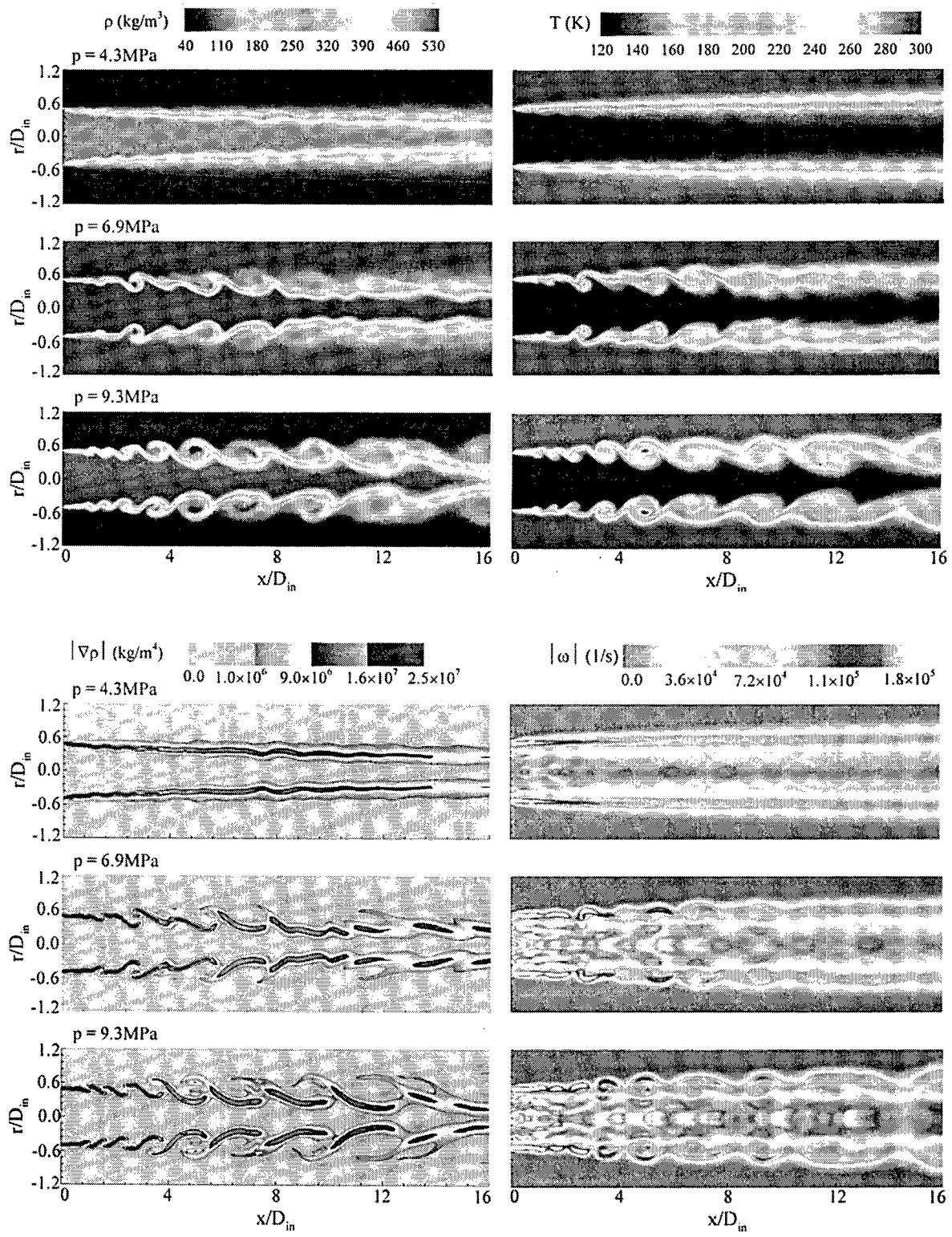

Fig. 3 Effect of pressure on density, temperature, density-gradient and vorticity fields (T_∞=300 K, u_{in}= 15 m/s, T_{in}= 120 K, D_{in}=254μm, t=1.550 ms).

Under this condition, most thermal energy transferred from the hot ambient gas to the cold jet is used to facilitate volume expansion. The injected fluid is only heated slightly as it moves downstream. However, the normalized density of Case 1 (in Fig. 4) decreases much faster along the jet centerline than that of Cases 2 and 3. The reason is obvious. At the present simulation conditions, the compressibility factor of nitrogen fluid decreases when the ambient pressure decreases. In Case 1, the relatively lower ambient pressure results in a smaller compressibility factor. Thus, a slight increase in temperature causes a large density decrease. Another unique phenomenon observed in Fig. 4 is that the normalized density decreases much more quickly than the normalized temperature in all three cases. As we have stated, when a fluid initially at the subcritical temperature is injected into a supercritical environment, it heats up and eventually exceeds the critical temperature of the fluid. At the critical temperature, the constant pressure specific heat of the nitrogen reaches its local maximum. Because the specific heat of nitrogen increases strikingly as the temperature of the jet fluid reaches the region near the critical temperature, the heat transferred from the ambient gas to the injected fluid is not primarily expended on temperature increase, but rather to facilitate the expansion of the jet flow. Therefore, the normalized temperature distribution along the jet centerline decreases very slowly. On the other hand, the compressibility factor of nitrogen varies very quickly with the temperature variation. Thus, a slight increase in the temperature of the injected fluid will cause the density of the jet to decrease largely.

CONCLUSIONS

A comprehensive numerical study has been conducted to investigate cryogenic fluid injection and mixing at supercritical conditions. The model accommodates full conservation laws and real-fluid thermodynamics and transport phenomena over the entire fluid states of concern. Turbulent closure is achieved using a large-eddy-simulation technique. The Major results obtained are summarized below.

1. The present analysis allows for a detailed investigation of the temporal and spatial evolution of cryogenic jets at supercritical conditions. The near-field dynamics of the turbulent jet is well captured.
2. As a result of turbulent mixing and property variations, a series of large density-gradient regions are generated around the jet surface. These regions act like a solid wall that amplifies the axial flow oscillations but damps the radial ones. The jet surface motions are effectively suppressed, especially for the case with large density ratios. As the ambient pressure increases, the strength of the initial density stratification decreases, so does it's damping effect. Therefore, the instability waves on the jet surface are much more evident in the case with a relatively higher pressure.
3. The jet dynamics is largely dictated by the local thermodynamic state. When the fluid temperature transits from a sub- to a super-critical value, rapid property variations may qualitatively change the jet behavior compared with its counterpart at low pressures.

ACKNOWLEDGEMENTS

This work was sponsored by the Air Force Office of Scientific Research, Grant No. F49620-01-1-0114. The author gratefully acknowledge the support from Dr. Mitat A. Birkan contract monitor of the program.

REFERENCES

Bellan, J., 2000, "Supercritical (and Subcritical) Fluid Behavior and Modeling: Drops, Streams, Shear and Mixing Layers, Jets and Sprays," *Progress in energy and combustion science*, Vol. 26, pp. 329-366.

Chehroudi, B., Cohn, R., Talley, D., and Badakhshan, A., 2000, "Raman Scattering Measurements in the Initial Region of Sub and Supercritical Jets," AIAA Paper No. 00-3392, 36th AIAA/ASME/SAE/ASEE Joint Propulsion Conference & Exhibit, Huntsville, AL, July 2000.

Chehroudi, B., Talley, D., and Coy, E., 2002a, "Visual Characteristic and Initial Growth Rate of Round Jets at Subcritical and Supercritical Pressure," *Physics of Fluids*, Vol. 114, pp. 850-861.

Chehroudi, B., and Talley, D., 2002b, "Interaction of Acoustic Wave with a Cryogenic Nitrogen Jet at Sub- and Supercritical Pressure," AIAA Paper No. 02-0342, 40th AIAA Aerospace Sciences Meeting and Exhibit, Reno, NV, January 2002.

Crow, S. C., and Champagne, F. H., 1971, "Orderly Structure in Jet Turbulence," *J. Fluid Mech.*, Vol. 48, pp. 547-591.

Hannoun, I. A., Fernando, H. J. S., and List, E. J., 1988, "Turbulent Structure Near a Sharp Density Interface," *J. Fluid Mech*, Vol 189, pp. 189-209.

Hsieh, S. Y., and Yang, V., 1997, "A Preconditioning Flux-Difference Scheme for Chemically Reacting Flows at all Mach Numbers," *International Journal of Computational Fluid Dynamics*, Vol. 8, pp. 31-49.

Levelt Senger, J. M. H., 1991, "Thermodynamics of Solutions near the Solvent's Critical Point," Supercritical Fluid Technology, Chapter 1, CRC Press, Inc, 1991, Boca Raton, Florida.

Mayer, W., Ivancic, A., Schik, A., and Hornung U., 1996, "Propellant Atomization in LOX/GH2 Rocket Combustors," AIAA Paper No. 96-3568, 34th AIAA/ASME/SAE/ASEE Joint Propulsion Conference & Exhibit, Reno, Nevada, January 1996.

Meng, H., and Yang, V., 2003, "A Unified Thermodynamics Treatment of General Fluid Mixtures and Its Application to a Preconditioning Scheme," to be published in Journal of Computational Physics.

Miller, S., and Bellan, J., 2002, "Direct Numerical Simulations of Supercritical Fluid Mixing Layers Applied to Heptane-Nitrogen," *J. Fluid Mech.*, Vol. 436, pp. 1-34.

Newman, J. A., and Brzustowski, T. A., 1971, "Behavior of a Liquid Jet near the Thermodynamic Critical Region," *AIAA J.*, Vol. 19, pp. 1595-1601.

Oefelein, J. C., and Yang, V., 1998, "Modeling High-Pressure Mixing and Combustion Processes in Liquid Rocket Engines," *Journal of Propulsion and Power*, Vol. 114, pp. 843-857.

Okong'o, N., Harstad, K., and Bellan J., 2002, "Direct Numerical Simulations of O_2/H_2 Temporal Mixing Layers Under Supercritical Conditions," *AIAA J.*, Vol. 40, pp. 914-926.

Oschwald, M., and Schik, A., 1999, "Supercritical Nitrogen Free Jet Investigated by Spontaneous Raman Scattering," *Experiments in Fluid*, Vol. 127, pp. 497-506.

Yang, V., 2000, "Modeling of Supercritical Vaporization, Mixing, and Combustion Processes in Liquid-Fueled Propulsion Systems," *Proceedings of Combustion Institute*, Vol. 28, pp. 925-942.